

# The Dirac- $\tau$ Unification



**Dirac's equation reinterpreted  
as geometry of a single scalar  
field of proper time  $\tau$ .**

# The Dirac- $\tau$ Unification: Spin, Mass, and Quantum Phase as Orientations of Proper-Time Flow

Dominik Kluczek  
(The Smart Fox)

December 2, 2025

## Abstract

We develop a unified geometric framework in which mass, spin, gravitation, and quantum phase emerge from a single underlying quantity: a dynamical proper-time field  $\tau(x)$ . By promoting  $\tau$  from a passive parameter to a scalar field with curvature, gradient, and oscillation, we show that matter waves arise as  $\tau$ -phase oscillations, momentum emerges from  $\partial_\mu\tau$ , and energy corresponds to  $\Delta\tau/\tau$ . The Dirac equation appears naturally as the first-order propagation law for the orientation of  $\tau$ -flow, expressed compactly as

$$(i\hbar\gamma^\mu\partial_\mu - mc)\psi = 0 \rightarrow \gamma^\mu\partial_\mu\tau\psi = \frac{1}{c}\psi,$$

revealing spin as the orientation of the  $\tau$ -gradient and mass as its internal oscillation frequency. Gravitation emerges as the long-range structure of  $\tau$ -curvature, and Planck-scale physics arises from nonlinear saturation of the  $\tau$ -field. The theory yields numerous experimental predictions including spin-dependent gravitational phase shifts, spin-split matter-wave interference, modified redshift scaling, enhanced zitterbewegung, and deviations in frame-dragging. These are all testable with current or near-future technology.



Figure 1: Visual signature of Okilmes.

# Contents

<b>1</b>	<b>Prelude on the Interpretation of <math>\tau</math></b>	<b>6</b>
<b>2</b>	<b>Introduction To The Time-Field Theory (TFT)</b>	<b>9</b>
<b>3</b>	<b>Core Concepts of TFT: <math>\tau</math>, <math>u</math>, and the <math>\tau</math>-Field Lagrangian</b>	<b>9</b>
3.1	The $u$ Reproduces Gravitational Potential . . . . .	10
3.2	The $u$ Determines Local Energy Density . . . . .	10
3.3	The $\tau$ -Field Lagrangian . . . . .	10
<b>4</b>	<b>Matter Waves as <math>\tau</math>-Phase Rotations</b>	<b>12</b>
4.1	Phase as $\tau$ -Accumulation . . . . .	12
4.2	The $\tau$ -Gradient Generates Momentum . . . . .	12
4.3	Schrödinger Equation as Low-Gradient Limit . . . . .	13
<b>5</b>	<b>Deriving the Dirac Equation from Oriented <math>\tau</math>-Flow</b>	<b>13</b>
5.1	From $\tau$ -Phase to the Relativistic Energy–Momentum Relation . . . . .	13
5.2	The Need for a First-Order Law . . . . .	14
5.3	The Square Root of $\tau$ -Geometry . . . . .	14
5.4	Interpretation: Spin as Orientation of $\tau$ -Gradient . . . . .	16
5.5	Positive and Negative Energy as Opposite $\tau$ -Orientations . . . . .	16
5.6	Zitterbewegung from $\tau$ -Orientation Interference . . . . .	17
5.7	Mass as the Torsion Frequency of Proper Time . . . . .	17
<b>6</b>	<b>Mass, Spin, Interference, and Frequency as <math>\tau</math>-Geometry</b>	<b>18</b>
6.1	Mass as the Oscillation Frequency of $\tau$ . . . . .	19
6.2	Momentum as Spatial Variation of $\tau$ . . . . .	19
6.3	Chirality and the $\tau$ -Field . . . . .	20
6.4	Spin as Orientation of $\tau$ -Flow . . . . .	20
6.5	Positive and Negative Energy as Forward/Backward $\tau$ -Phase Rotation . . . . .	21
6.6	The Complex Nature of Quantum Amplitudes . . . . .	21
6.7	Zitterbewegung as Interference of Opposite $\tau$ -Orientations . . . . .	22
6.8	Wave–Particle Duality as a Single Field Property . . . . .	22
6.9	Why the Dirac Equation Must Be First-Order . . . . .	22
6.10	The Bridge Between Relativity and Quantum Mechanics . . . . .	23
<b>7</b>	<b>Predictions and Experimental Tests of the <math>\tau</math>-Dirac Framework</b>	<b>23</b>
7.1	Spin– $\tau$ Coupling Effects . . . . .	23
7.1.1	Spin-Dependent Phase Accumulation . . . . .	23
7.1.2	Spin Precession in Weak Gravitational Gradients . . . . .	24
7.1.3	Gravitational Birefringence for Matter Waves . . . . .	24
7.2	Interferometric and Phase-Based Phenomena . . . . .	24
7.2.1	Spin-Split Double-Slit Interference . . . . .	25
7.2.2	Enhanced Zitterbewegung Observability . . . . .	25

7.3	Spectroscopic and Mass-Frequency Shifts . . . . .	25
7.3.1	Mass Shifts in Atomic Energy Levels . . . . .	25
7.3.2	Spin-Dependent Redshift in Spectroscopy . . . . .	25
7.4	Macroscopic and Relativistic Predictions . . . . .	25
7.4.1	Correction to Lense–Thirring Frame Dragging . . . . .	25
7.4.2	Gravitational Decoherence Scaling with $\tau$ -Gradient . . . . .	26
7.4.3	Matter-Wave Time Delay Across $\tau$ -Flow Discontinuities . . . . .	26
7.5	Summary of Unique Predictions . . . . .	26
<b>8</b>	<b>Experimental Proposals to Test the <math>\tau</math>–Dirac Framework</b>	<b>27</b>
8.1	Near-Term Feasible Experiments . . . . .	27
8.1.1	Spin-Split Atom Interferometry (Primary Clean Test) . . . . .	27
8.1.2	Hyperfine Spectroscopy in Variable Gravitational Potential . . . . .	28
8.1.3	Spin-Dependent Free-Fall of Neutrons . . . . .	28
8.1.4	Graphene Dirac Cone Zitterbewegung . . . . .	28
8.2	Mid-Term Experiments . . . . .	28
8.2.1	Satellite–Ground Entanglement Decay . . . . .	28
8.2.2	Atom Interferometry in Microgravity . . . . .	29
8.2.3	Spin–Frame-Dragging Detection . . . . .	29
8.3	Long-Term Ambitious Experiments . . . . .	29
8.3.1	Direct Mapping of the $\tau$ -Field . . . . .	29
8.3.2	Spin-Engineered Neutrino Gravitational Lensing . . . . .	29
8.3.3	$\tau$ -Orientation in Binary Black Hole Systems . . . . .	29
8.4	Summary of the Experimental Program . . . . .	29
<b>9</b>	<b>Experimental Access to Temporal Curvature and Torsion</b>	<b>30</b>
9.1	Measuring Temporal Curvature $u$ . . . . .	30
9.2	Measuring Temporal Torsion (Mass-Linked Twist) . . . . .	30
9.3	Flagship Test of Spin-Resolved Atom Interferometry . . . . .	31
<b>10</b>	<b>Discussion and Outlook</b>	<b>32</b>
10.1	Conceptual Shift: From Spacetime to Timeflow Geometry . . . . .	32
10.2	Compatibility with General Relativity . . . . .	32
10.3	Compatibility with Quantum Mechanics . . . . .	33
10.4	Implications for Quantum Gravity . . . . .	33
10.5	Relation to Dirac Theory in Curved Spacetime . . . . .	33
10.6	Cosmological Implications and Observational Tests . . . . .	34
10.7	Planck Physics: A Natural Saturation Mechanism . . . . .	35
10.8	Open Research Directions . . . . .	35
<b>11</b>	<b>Conclusion</b>	<b>36</b>
<b>12</b>	<b>Unification Table Summary</b>	<b>37</b>

<b>13 Appendix Derivations in <math>\tau</math>-Field Geometry</b>	<b>39</b>
<b>A From <math>\tau</math>-Phase to the Klein–Gordon Equation</b>	<b>39</b>
<b>B From the Mass Shell to the <math>\tau</math>-Gradient Constraint</b>	<b>40</b>
<b>C Dirac as a First-Order Law for Oriented <math>\tau</math>-Flow</b>	<b>40</b>
<b>D Weak-Field Limit and Relation to Gravitational Potential</b>	<b>42</b>
<b>E Planck-Scale Saturation of the <math>\tau</math>-Field</b>	<b>42</b>
<b>F Numerical Illustration of the <math>\tau</math>-Dirac Mapping</b>	<b>43</b>
F.1 1+1D Dirac Plane Waves and the Timeflow Vector . . . . .	43
F.2 Interference of $\pm\tau$ -Phases and Zitterbewegung . . . . .	44
F.3 Python Reference Implementation . . . . .	46

# 1 Prelude on the Interpretation of $\tau$

Although the present work treats proper time  $\tau(x)$  as a physical field, we stress that this is fully compatible with general relativity (GR) and standard quantum mechanics (QM). In the weak-field limit of GR, the gravitational redshift relation gives

$$\frac{\Delta\tau}{\tau} = \frac{\Phi}{c^2}, \quad (1)$$

so the dimensionless curvature

$$u \equiv \frac{\Delta\tau}{\tau} \quad (2)$$

may be interpreted equivalently as gravitational potential or temporal curvature. Nothing in the analysis to follow contradicts verified GR predictions. Rather,  $\tau$ -geometry extends GR by giving a physical interpretation to proper-time flow and applying it to the domain of relativistic quantum mechanics.

This framing allows to remain grounded in familiar gravitational intuition while exploring the richer consequences of  $\tau$ -geometry. TFT is still new concept and is yet to be subjected to review and formal scrutiny. With that in mind lets us continue.

## Guided Overview (Non-Technical Summary)

For readers less familiar with the complex formalism, we briefly summarize the core idea in more intuitive language. Where in standard physics, time is usually treated as a coordinate: a label that orders events. In the present framework, we instead treat *proper time*  $\tau(x)$  as a physical field that can bend, twist, and oscillate. The central claim is that many familiar quantities in physics are different aspects of this time-field:

- Gravitation corresponds to how fast  $\tau$  runs in different places (curvature of the time-field).
- Quantum waves correspond to oscillations of the phase  $\omega\tau(x)$ .
- Mass corresponds to how quickly the time-field twists between two internal “sheets” of the field (a torsion rate).
- Spin corresponds to the orientation of this internal time twist.

The Dirac equation, which normally describes relativistic particles with spin, can then be re-interpreted as a first-order law describing how this time-field flows and twists. The rest of the paper develops this interpretation in full mathematical detail and shows how it reproduces standard results while suggesting new experimental signatures.

## Definition of Timeflow

In this work, “timeflow” refers to the geometric structure induced by the proper-time field  $\tau(x)$  and its gradient. We define

$$T_\mu(x) \equiv \partial_\mu \tau(x), \quad (3)$$

and, in regions where  $T_\mu T^\mu > 0$ , the normalized timeflow vector

$$t^\mu(x) \equiv \frac{T^\mu}{\sqrt{T_\alpha T^\alpha}}. \quad (4)$$

In the  $\tau$ -Dirac framework, the mass-shell condition enforces

$$T_\mu T^\mu = \frac{1}{c^2}, \quad (5)$$

so that  $t^\mu = c T^\mu$  is a unit timelike vector field. The level sets  $\tau(x) = \text{const.}$  define a local foliation of spacetime by hypersurfaces of equal proper time, while  $t^\mu$  defines the local direction of increasing proper time.

Importantly,  $\tau$  is not introduced as a preferred global coordinate or external time parameter. Instead, it is a scalar field that can, in principle, be operationally reconstructed from a congruence of ideal clocks. The “timeflow” is therefore a geometric and physical object, not a choice of gauge.

## Directionality of Timeflow

Given the gradient  $T_\mu = \partial_\mu \tau$ , the timeflow vector  $t^\mu = c T^\mu$  has a natural orientation: it points in the direction of increasing proper time. Locally, we select the branch

$$t^0 > 0, \quad (6)$$

which enforces that  $\tau$  increases along physical worldlines in the same sense as standard thermodynamic and cosmological arrows of time.

This choice does not introduce a new preferred frame: it is equivalent to the usual selection of a future-directed timelike direction in relativistic field theory. All equations in the bulk remain covariant under Lorentz transformations; the arrow of time is encoded in the sign choice of  $t^\mu$  and in boundary conditions (such as  $\tau \rightarrow +\infty$  along expanding cosmological worldlines), rather than in any explicit breaking of Lorentz symmetry.

Where the sign of  $t^\mu$  matters (for example, in distinguishing particle from antiparticle or left-handed from right-handed modes), it appears as the sign of the  $\tau$ -torsion and is reflected in the relative orientation of the two sheets of the spinor structure.

## Notation and Assumptions

These assumptions are made explicit so that the domain of validity of each derivation can be clearly assessed. We work in a  $(+, -, -, -)$  metric signature with  $\eta^{\mu\nu} = \text{diag}(1, -1, -1, -1)$  and keep  $c$  and  $\hbar$  explicit where this aids interpretation. Greek indices  $\mu, \nu, \dots$  run over spacetime components  $0, 1, 2, 3$ .

The proper-time field is a scalar  $\tau(x)$ , with gradient

$$T_\mu(x) \equiv \partial_\mu \tau(x), \quad (7)$$

and dimensionless curvature

$$u(x) \equiv \frac{\Delta\tau}{\tau}. \quad (8)$$

In the weak-field limit we have  $u \approx \Phi/c^2$ , so  $u$  may be regarded as a generalized gravitational potential. With that we assume throughout:

**A1**  $\tau(x)$  is a smooth Lorentz scalar field.

**A2** In the regimes of interest the wavefunction can be written as

$$\psi(x) = A(x) e^{i\omega\tau(x)},$$

with a slowly varying envelope  $A(x)$  such that derivatives of  $A(x)$  are subleading compared to derivatives of the phase.

**A3** On the mass shell of a free particle, the timeflow vector satisfies

$$T_\mu T^\mu = \frac{1}{c^2},$$

corresponding to a unit timelike direction (in units where  $c = 1$ ).

## Timeflow and Lorentz Covariance

The “timeflow” in this work is not a preferred global time coordinate, but the local geometric object built from  $\tau$  and its gradient. We define the timeflow vector

$$t^\mu(x) \equiv c T^\mu(x) = c \partial^\mu \tau(x), \quad (9)$$

which, under Assumption A3, satisfies  $t_\mu t^\mu = 1$  for a free massive particle. The level sets  $\tau(x) = \text{const.}$  define local hypersurfaces of equal proper time, and  $t^\mu$  points along the future-directed timelike direction in which  $\tau$  increases. All fundamental equations in this paper are Lorentz covariant:  $\tau(x)$  transforms as a scalar,  $T_\mu$  and  $t^\mu$  as vectors, and the Dirac operator retains its usual Clifford algebra. The choice of the future-directed branch  $t^0 > 0$  encodes the usual arrow of time, but does not introduce any new preferred frame beyond standard relativistic conventions.

## 2 Introduction To The Time-Field Theory (TFT)

In classical physics, proper time is an inert parameter. The Time-Field Theory (TFT) promotes  $\tau(x)$  to a field with geometric and dynamical content. Its curvature, gradient, and oscillatory structure encode energy, momentum, wave behavior, and internal frequency.

The core identities of TFT are:

- Energy  $\rightarrow E \sim c^2 \Delta\tau/\tau$
- Momentum  $\rightarrow p_\mu = \hbar\omega \partial_\mu \tau$
- Phase  $\rightarrow \phi = \omega\tau(x)$
- Spin  $\rightarrow$  orientation of  $\partial_\mu \tau$

The dimensionless curvature field

$$u = \frac{\Delta\tau}{\tau} \quad (10)$$

reproduces gravitational redshift for  $u \ll 1$ , yet extends naturally into nonlinear regimes relevant to quantum and Planck-scale dynamics.

From this field, the core structures of physics emerge:

- Energy arises from curvature of  $\tau$ .
- Momentum arises from spatial gradients of  $\tau$ .
- Mass is the frequency of internal  $\tau$ -phase rotation.
- Wave behavior results from interference of  $\tau$ -phase along different paths.
- Gravitation is the long-range gradient of  $\tau$ .
- Quantization results from closed  $\tau$ -loops (phase closure conditions).
- Planck physics appears as saturation of  $\tau$ -curvature.

## 3 Core Concepts of TFT: $\tau$ , $u$ , and the $\tau$ -Field Lagrangian

The Time-Field Theory (TFT) begins from a minimal assumption:

Proper time  $\tau(x)$  is not merely a coordinate parameter but a physical field defined over spacetime.

Everything that follows emerges from this.

The field  $\tau(x)$  carries three essential structures:

- **Curvature** → how  $\tau$  accelerates or decelerates (energy).
- **Gradient** → how  $\tau$  differs between neighboring points (momentum, gravitation).
- **Phase** → how  $\tau$  contributes to oscillatory behavior (quantum interference).

To work in dimensionless units, we introduce the normalized curvature field:

$$u(x) = \frac{\Delta\tau}{\tau}. \quad (11)$$

This ratio is the central object of TFT and has three crucial properties.

### 3.1 The $u$ Reproduces Gravitational Potential

In the weak-field limit of general relativity, the gravitational redshift relation gives:

$$\frac{\Delta\tau}{\tau} = \frac{\Phi}{c^2} \rightarrow u = \frac{\Phi}{c^2}.$$

The  $\tau$ -field generalizes gravitational potential, rather than replacing it. This equivalence ensures that TFT preserves all validated predictions of GR in regimes where  $\Phi/c^2 \ll 1$ .

### 3.2 The $u$ Determines Local Energy Density

An accelerated or compressed  $\tau$ -flow stores energy. The normalized curvature  $u$  therefore measures:

$$u \propto \text{local temporal energy density}.$$

In previous TFT work, this led directly to the mass–energy relation:

$$E = c^2 \frac{\Delta\tau}{\tau},$$

showing that energy arises from compression of  $\tau$ .

This formula becomes the geometric bridge between mass, gravitational potential, and quantum frequency.

### 3.3 The $\tau$ -Field Lagrangian

The dynamics of  $\tau$  are captured by the Lagrangian density:

$$\mathcal{L}_\tau = \frac{c^4}{8\pi G} (\partial_\mu u)(\partial^\mu u) - \rho c^2 u - \frac{\kappa}{3} u(\partial_\mu u)(\partial^\mu u).$$

Each term plays a distinct role:

- **Kinetic term:**

$$\frac{c^4}{8\pi G}(\partial_\mu u)(\partial^\mu u)$$

governs propagation of  $\tau$ -gradients and reproduces Newtonian gravity in the small-gradient limit.

- **Matter coupling:**

$$-\rho c^2 u$$

couples  $\tau$ -curvature to mass density, yielding the Poisson equation in weak fields and the Einstein redshift factor.

- **Self-interaction term:**

$$-\frac{\kappa}{3} u(\partial_\mu u)(\partial^\mu u)$$

accounts for nonlinearities that become significant near  $u \rightarrow 1$ , encoding Planck-scale behavior.

The Euler–Lagrange equation yields a second-order scalar equation:

$$\square u - \kappa(u\square u + \partial_\mu u \partial^\mu u) = 4\pi G\rho,$$

a nonlinear Klein–Gordon–type structure governing the magnitude of  $\tau$ -curvature. This equation controls the *scalar* content of  $\tau$ : its slope, curvature, and saturation. However, matter does not respond only to the *magnitude* of  $\tau$ -curvature →. it also responds to its **orientation**.

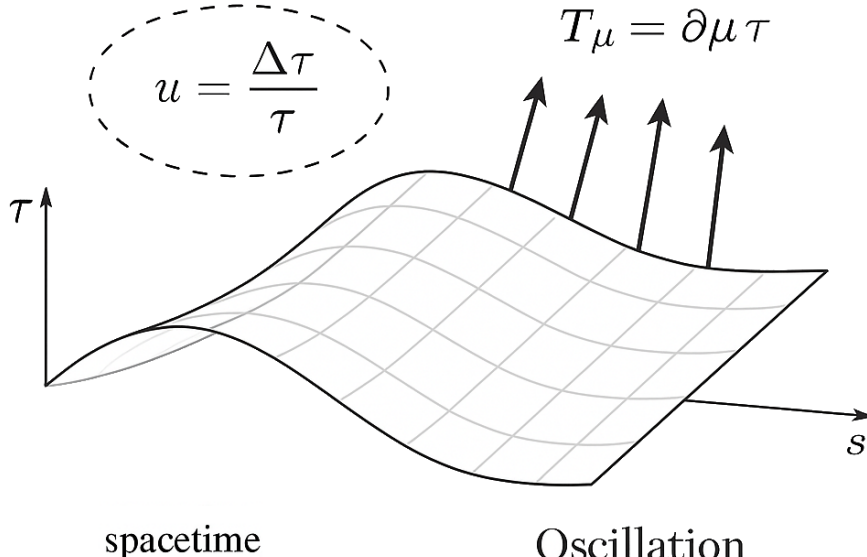


Figure 2: Schematic illustration of the proper-time field  $\tau(x)$  as a scalar field with curvature  $u = \Delta\tau/\tau$  and gradient  $T_\mu = \partial_\mu\tau$ . Curvature encodes energy, and gradient encodes momentum and gravitational potential.

## 4 Matter Waves as $\tau$ -Phase Rotations

Quantum theory describes matter as waves with complex phase:

$$\psi = A(x) e^{i\phi(x)}.$$

In TFT, the phase is purely temporal:

$$\phi(x) = \omega \tau(x).$$

This is not symbolic notation as it is a physical identity.

### 4.1 Phase as $\tau$ -Accumulation

A particle's phase increases with proper-time flow. If two paths accumulate different  $\tau$ , the phase difference is

$$\Delta\phi = \omega \Delta\tau,$$

directly producing interference. This explains quantum fringes without invoking probability axioms: interference is simply the difference in accumulated  $\tau$ -phase.

### 4.2 The $\tau$ -Gradient Generates Momentum

Differentiating the wavefunction,

$$\partial_\mu \psi = i\omega(\partial_\mu \tau) \psi + (\partial_\mu A) e^{i\omega\tau}.$$

In regions where the envelope  $A(x)$  varies slowly,

$$\partial_\mu \psi \approx i\omega(\partial_\mu \tau) \psi.$$

This approximation is valid when the  $\tau$ -phase varies on spacetime scales much shorter than the envelope  $A(x)$ , for example for high-frequency modes or slowly modulated wave packets. In this WKB-like regime, the phase term  $i\omega(\partial_\mu \tau)\psi$  dominates the derivative, while the envelope derivative  $\partial_\mu A$  gives only subleading corrections. A full derivation and the precise conditions under which this limit holds are worked out in Appendix A. Meanwhile we define momentum via

$$p_\mu = \hbar \omega \partial_\mu \tau.$$

This reproduces:

- the de Broglie relation,
- the geometric optics limit of wave propagation,
- and the standard identity  $p_\mu = \partial_\mu \phi$ .

It also ties momentum to geometry rather than abstraction as **momentum is how fast  $\tau$  changes in space**.

### 4.3 Schrödinger Equation as Low-Gradient Limit

Expanding  $\tau(x)$  for slowly varying fields,

$$\tau(x + \delta x) \approx \tau(x) + \frac{\partial_i \tau}{\partial t} \delta x^i,$$

leads to the Schrödinger equation when velocities are small and  $\nabla \tau \ll 1$ . Where, quantum mechanics emerges as **the low-gradient, low-curvature evolution of  $\tau$ -phase**.

## 5 Deriving the Dirac Equation from Oriented $\tau$ -Flow

The preceding sections established that a matter wave may be written as a pure  $\tau$ -phase oscillation:

$$\psi(x) = A(x) e^{i\omega \tau(x)}.$$

In regions where the envelope varies slowly,

$$\partial_\mu \psi \approx i\omega (\partial_\mu \tau) \psi.$$

Define the  $\tau$ -gradient:

$$T_\mu \equiv \partial_\mu \tau,$$

and the  $\tau$ -momentum:

$$p_\mu = \hbar\omega T_\mu.$$

This simple identity contains the seeds of the Dirac equation.

### 5.1 From $\tau$ -Phase to the Relativistic Energy–Momentum Relation

A free massive particle satisfies:

$$\eta^{\mu\nu} p_\mu p_\nu = m^2 c^2.$$

Substituting  $p_\mu = \hbar\omega T_\mu$  gives:

$$(\hbar\omega)^2 \eta^{\mu\nu} T_\mu T_\nu = m^2 c^2.$$

This is the scalar (Klein–Gordon) constraint written purely in  $\tau$ -geometry:

$$\eta^{\mu\nu} \partial_\mu \tau \partial_\nu \tau = \frac{m^2 c^2}{(\hbar\omega)^2} = \frac{1}{c^2}. \quad (12)$$

The second equality holds because for a bound excitation,

$$\hbar\omega = mc^2,$$

the familiar rest-energy relation. In this section we have fixed  $\hbar\omega = mc^2$  to emphasize the rest-frame identification of mass with the internal torsion frequency of  $\tau$ . For a general moving excitation one may regard  $\omega$  as the rest-frame frequency and allow the full four-momentum  $p_\mu$  to enter through the usual dispersion relation, with  $\tau$ -phase depending on  $p_\mu x^\mu$ . The timelike vector  $T_\mu$  then aligns with the normalized four-velocity associated with that excitation.

$$\eta^{\mu\nu} T_\mu T_\nu = \frac{1}{c^2}.$$

So the  $\tau$ -gradient is a **unit timelike vector** rescaled by the speed of light. This relation encodes the *magnitude* of the  $\tau$ -flow. What it lacks is **orientation**. Magnitude alone cannot describe spin.

## 5.2 The Need for a First-Order Law

The Klein–Gordon equation,

$$\left( \square + \frac{m^2 c^2}{\hbar^2} \right) \psi = 0,$$

is second order in derivatives. It constrains the magnitude of the four-momentum but cannot encode the orientation of a directed quantity like  $T_\mu$ . Yet quantum matter (electrons, neutrinos, quarks) possesses spin, a property fundamentally tied to orientation. The theory must be completed by a first-order equation whose square reproduces the Klein–Gordon magnitude constraint.

Dirac uniquely constructed such an operator:

$$(i\hbar\gamma^\mu \partial_\mu - mc) \psi = 0,$$

whose square yields the Klein–Gordon operator component-wise.

Within TFT, this operator arises naturally when  $\tau$ -flow is given orientation.

## 5.3 The Square Root of $\tau$ -Geometry

Substitute the  $\tau$ -gradient identity:

$$\partial_\mu \psi \approx i\omega T_\mu \psi,$$

into Dirac's operator:

$$i\hbar\gamma^\mu \partial_\mu \psi = -\hbar\omega \gamma^\mu T_\mu \psi.$$

The Dirac equation becomes:

$$-\hbar\omega \gamma^\mu T_\mu \psi - mc\psi = 0.$$

Using  $\hbar\omega = mc^2$ :

$$-mc^2 \gamma^\mu T_\mu \psi - mc\psi = 0.$$

Divide by  $mc$ :

$$-c \gamma^\mu T_\mu \psi = \psi.$$

Or equivalently:

$$\boxed{\gamma^\mu T_\mu \psi = -\frac{1}{c} \psi} \quad (13)$$

Up to an irrelevant sign (absorbed into conventions), this is the compact TFT–Dirac identity:

$$\boxed{\gamma^\mu \partial_\mu \tau \psi = \frac{1}{c} \psi} \quad (14)$$

This equation is the **first-order law for oriented  $\tau$ -flow**. (see figure 3 for schematic of this dual-sheet torsional structure).

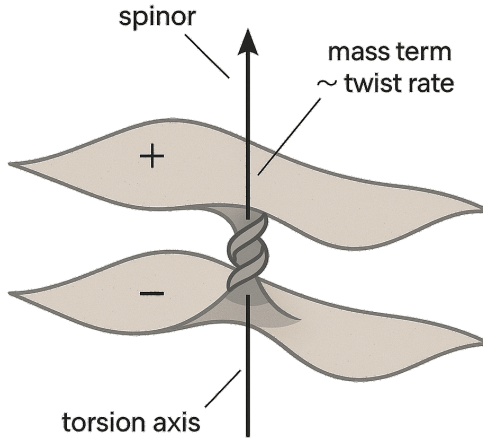


Figure 3: **Schematic of the Dirac Spinor in a  $\tau$ -Field Geometry.** The spinor is modeled as a two-sheet structure on a folded proper-time manifold. Positive and negative frequency components appear as separate  $\tau$ -field sheets separated by a torsional axis; the  $\pm$  orientation encodes spin-helicity; mass arises from the twist rate that couples the two sheets (untwisted  $\rightarrow$  massless fermion, twisted  $\rightarrow$  massive fermion); the central torsion line represents intrinsic chirality and unidirectional temporal flow determining particle/antiparticle identity.

## 5.4 Interpretation: Spin as Orientation of $\tau$ -Gradient

The equation above states:

The  $\gamma$ -matrices project the  $\tau$ -gradient into the spinor, enforcing a specific orientation of  $\tau$ -flow for a given mass.

The  $\gamma$ -matrices form a basis of the Clifford algebra the unique algebra whose square yields the Minkowski metric.

There for:

- The **magnitude** of  $T_\mu$  enforces the relativistic mass shell.
- The **orientation** of  $T_\mu$  determines the spin state.

Spin as an intrinsic quantum attribute in TFT, viewed rather as:

**The orientation of proper-time flow in spacetime, lifted to the double-cover representation  $\text{Spin}(1, 3)$ .**

This could resolve several classical puzzles:

- why spin has no classical analogue,
- why spinors require  $4\pi$ , not  $2\pi$ , to return to identity,
- why electrons exhibit intrinsic magnetic moment,
- why matter waves have complex structure,
- why Dirac requires both positive and negative energy solutions.

All arise because the  $\tau$ -gradient is **geometrically oriented**, and orientation must be represented on a double-cover group.

## 5.5 Positive and Negative Energy as Opposite $\tau$ -Orientations

The Dirac dispersion relation splits into two branches:

$$E = +\sqrt{m^2 c^4 + p^2 c^2}, \quad E = -\sqrt{m^2 c^4 + p^2 c^2}.$$

Traditionally interpreted as:

- antiparticles,
- negative energy sea,
- particle-hole excitations.

In TFT the picture is simpler:

$$\psi_{\pm} \sim e^{\pm i\omega\tau}.$$

The  $\pm$  corresponds to the **orientation of  $\tau$ -phase rotation**:

- forward rotation  $\rightarrow$  positive energy,
- backward rotation  $\rightarrow$  negative energy.

This geometrizes charge conjugation. No metaphysical “sea” is needed  $\rightarrow$  only reversed  $\tau$ -rotation. Which in contact with each other symmetrically canceling phase releasing great amounts of energy  $\rightarrow$  releasing the tension at once.

## 5.6 Zitterbewegung from $\tau$ -Orientation Interference

The oscillation known as *zitterbewegung*, predicted but elusive, corresponds to interference between the two  $\tau$ -orientation branches:

$$\psi = \psi_+ + \psi_- = e^{i\omega\tau} + e^{-i\omega\tau} = 2 \cos(\omega\tau).$$

The trembling motion arises from:

### Beating between opposite orientations of $\tau$ -phase flow.

TFT predicts this is physically real and detectable under appropriate conditions (see following Sections).

## 5.7 Mass as the Torsion Frequency of Proper Time

In the  $\tau$ -field picture, mass is not a fundamental scalar but the *torsion frequency* of proper time. This becomes explicit when we write the Dirac spinor in the phase form

$$\psi(x) = A(x) e^{i\omega\tau(x)}, \quad \hbar\omega = mc^2. \quad (15)$$

The quantity

$$\Theta \equiv \frac{d\phi}{d\tau} = \omega = \frac{mc^2}{\hbar} \quad (16)$$

is the intrinsic torsion rate of the  $\tau$ -field. Where

$$m = \frac{\hbar}{c^2} \Theta, \quad (17)$$

and mass is identified with the internal twist of proper time. A massless field corresponds to  $\Theta = 0$  and therefore to a flat (untwisted)  $\tau$  structure, consistent with propagation along null directions. Using the approximation  $\partial_\mu\psi \approx i\omega(\partial_\mu\tau)\psi$ , the Dirac equation

$$(i\hbar\gamma^\mu\partial_\mu - mc)\psi = 0 \quad (18)$$

reduces to the geometric identity

$$\gamma^\mu (\partial_\mu \tau) \psi = \frac{1}{c} \psi, \quad (19)$$

which describes the projection of the oriented  $\tau$ -gradient into spinor space. Squaring both sides recovers the constraint

$$(\partial_\mu \tau)(\partial^\mu \tau) = \frac{1}{c^2}, \quad (20)$$

showing that the Dirac operator acts as the “square root” of the  $\tau$ -metric. This interpretation leads directly to several physical consequences: zitterbewegung as beating between the  $\pm \omega$  torsion modes, the Compton wavelength as the natural folding scale of twisted  $\tau$ , and inertial mass as the resistance to reorientation of the  $\tau$ -flow. In the limit  $m \rightarrow 0$ , the torsion vanishes,  $\omega \rightarrow 0$ , and the Dirac equation reduces to the Weyl equation with conformal propagation.

## 6 Mass, Spin, Interference, and Frequency as $\tau$ -Geometry

With the  $\tau$ -Dirac equation in hand,

$$\gamma^\mu \partial_\mu \tau \psi = \frac{1}{c} \psi,$$

we can now translate each quantum property into geometric structure of the  $\tau$ -field. The result is a unified interpretation in which matter, energy, and spin arise from coherent features of oriented proper-time flow. The geometric identity used above is obtained by inserting a  $\tau$ -phase ansatz into the Dirac equation and working in a slowly varying envelope regime. For clarity, we write the spinor as:

$$\psi(x) = A(x) e^{i\omega\tau(x)}, \quad \hbar\omega = mc^2, \quad (21)$$

so that

$$\partial_\mu \psi = (\partial_\mu A) e^{i\omega\tau} + i\omega A(\partial_\mu \tau) e^{i\omega\tau}. \quad (22)$$

In the regime where the envelope  $A(x)$  varies slowly compared to the rapid  $\tau$ -phase, the second term dominates and we approximate

$$\partial_\mu \psi \approx i\omega(\partial_\mu \tau) \psi, \quad (23)$$

with relative corrections of order

$$\frac{|\partial_\mu A|}{|\omega| |\partial_\mu \tau| |A|}. \quad (24)$$

Substituting into the free Dirac equation

$$(i\hbar\gamma^\mu \partial_\mu - mc)\psi = 0 \quad (25)$$

gives

$$i\hbar\gamma^\mu \partial_\mu \psi \approx i\hbar\gamma^\mu [i\omega(\partial_\mu \tau)\psi] = -\hbar\omega \gamma^\mu (\partial_\mu \tau)\psi. \quad (26)$$

Using  $\hbar\omega = mc^2$ , we obtain

$$-mc^2 \gamma^\mu (\partial_\mu \tau)\psi - mc\psi \approx 0, \quad (27)$$

or, for  $m \neq 0$ ,

$$\gamma^\mu (\partial_\mu \tau) \psi \approx \frac{1}{c} \psi. \quad (28)$$

In the main text we use this as the leading-order geometric relation, understanding that it holds in the WKB-like regime where the  $\tau$ -phase dominates the spinor variation.

### 6.1 Mass as the Oscillation Frequency of $\tau$

Quantum mechanics introduces mass through the multiplicative term  $mc$  in the Dirac equation, but provides no fundamental explanation for its origin.

In TFT, mass becomes:

$$m = \frac{\hbar\omega}{c^2},$$

where  $\omega$  is the *internal  $\tau$ -phase frequency*. That allows us to view:

- a particle's mass = the rate at which its proper-time field oscillates;
- rest energy ( $mc^2$ ) = energy of this oscillation;
- mass is not a substance, but *temporal curvature trapped in place*.

This reframes mass as an emergent frequency property, not a stored quantity.

It naturally explains:

- Compton wavelength,
- quantum rest-energy,
- frequency–mass duality,
- why “massless” particles correspond to linear  $\tau$ -flow ( $\omega \rightarrow 0$ ).

### 6.2 Momentum as Spatial Variation of $\tau$

Momentum emerges from:

$$p_\mu = \hbar\omega \partial_\mu \tau.$$

This gives a direct geometric meaning: **Momentum is the spatial slope of the proper-time field.** Allowing us to view:

- particles move because  $\tau$  tilts;
- forces appear as local curvature of  $\tau$ ;
- acceleration arises from gradients in  $\partial_\mu \tau$ .

This collapses Newtonian, relativistic, and quantum concepts of momentum into a single expression.

### 6.3 Chirality and the $\tau$ -Field

Chiral symmetry is naturally expressed in terms of the operator

$$\gamma^5 = i\gamma^0\gamma^1\gamma^2\gamma^3, \quad (29)$$

which projects the Dirac spinor into left- and right-handed components

$$\psi_{L,R} = \frac{1 \mp \gamma^5}{2} \psi. \quad (30)$$

In the  $\tau$ -field picture, the two chiral components correspond to two distinct orientations of the timeflow with respect to the internal spinor sheets. The bilinear

$$\bar{\psi}\gamma^5\psi \quad (31)$$

may be interpreted as a pseudoscalar measuring the handedness of  $\tau$ -torsion relative to spatial directions.

In the massless limit ( $m \rightarrow 0$ ), the torsion frequency  $\Theta \rightarrow 0$  and the two chiralities decouple, recovering exact chiral symmetry as in the standard Weyl theory. For  $m \neq 0$ , chiral symmetry is broken by the finite twist rate of  $\tau$ , which couples left- and right-handed components and generates the usual Dirac mass term. This provides a geometric interpretation of chiral symmetry breaking: it is not merely an algebraic feature of the Dirac operator but a reflection of how the internal two-sheet structure of proper time is twisted in spacetime.

A deeper analysis of chiral anomalies and parity-violating interactions in this framework is left for future work, but the geometry of  $\tau$  clearly offers additional structure that could be relevant for understanding the origin and universality of chirality in fundamental interactions.

### 6.4 Spin as Orientation of $\tau$ -Flow

Spin is historically one of the most mysterious intrinsic properties of matter. Standard quantum theory treats it as a representation-theoretic requirement, not a physical phenomenon.

**In TFT: Spin is the orientation of the  $\tau$ -gradient embedded in the Clifford algebra.**

The  $\tau$ -gradient

$$T_\mu = \partial_\mu \tau,$$

has a direction in spacetime. The algebra of directions must be represented on the spinor double-cover  $\text{Spin}(1, 3)$ . Which makes:

- magnitude of  $T_\mu \rightarrow$  relativistic mass-shell;
- orientation of  $T_\mu \rightarrow$  spin state.

This interpretation explains:

- the  $720^\circ$  rotation property,
- intrinsic magnetic moment,
- spin–statistics connection,
- chirality and helicity,
- the necessity of four-component spinors in 3+1 dimensions.

No additional quantum postulates are required.

## 6.5 Positive and Negative Energy as Forward/Backward $\tau$ -Phase Rotation

Dirac's equation contains negative-energy states. In TFT these arise from reversed  $\tau$ -phase orientation:

$$\psi_+ \sim e^{+i\omega\tau}, \quad \psi_- \sim e^{-i\omega\tau}.$$

Wehre:

- positive energy = forward rotation of  $\tau$ ,
- negative energy = backward rotation of  $\tau$ .

Charge conjugation becomes: **the transformation  $\tau \rightarrow -\tau$  in the phase, inducing  $\psi \rightarrow \psi^* \gamma^2$  (Dirac basis).**

## 6.6 The Complex Nature of Quantum Amplitudes

Standard quantum mechanics assumes wavefunctions are complex.

Where TFT can offer an explanation why:

**Complex amplitudes encode rotation of  $\tau$ -phase.**

A purely real wave is a degenerate  $\tau$ -rotation with no orientation.

Complex exponentials convey:

- $\text{Re}(\psi)$  = projection of  $\tau$ -phase on one axis,
- $\text{Im}(\psi)$  = projection on orthogonal axis,
- $|\psi|$  = local envelope,
- $\arg(\psi)$  =  $\tau$ -phase.

The concept of complex wavefunctions resolves to:

*quantum phase is time rotating in a plane orthogonal to physical motion.*

## 6.7 Zitterbewegung as Interference of Opposite $\tau$ -Orientations

Standard QM predicts electron trembling at frequency  $2mc^2/\hbar$ , with limited physical interpretation.

In TFT:

$$\psi = e^{i\omega\tau} + e^{-i\omega\tau} = 2 \cos(\omega\tau),$$

so high-frequency oscillation is:

**interference between opposite orientations of  $\tau$ -phase flow.**

TFT can predict:

- zitterbewegung is real and measurable,
- it manifests as modulation in  $\tau$ -phase,
- it intensifies near strong  $\tau$ -curvature boundaries.

## 6.8 Wave–Particle Duality as a Single Field Property

Within TFT, the duality dissolves:

- **Wave nature** arises from interference of  $\tau$ -phase along multiple paths.
- **Particle nature** arises from stable  $\tau$ -curvature ( $u$ ) concentrated in localized regions.

A particle is a coherent  $\tau$ -mode; a wave is its distributed  $\tau$ -phase. They are not distinct objects, but different manifestations of  $\tau$ .

## 6.9 Why the Dirac Equation Must Be First-Order

The  $\tau$ -field equation governing  $u$  is second-order (Klein–Gordon-like), capturing magnitude. But direction requires a first-order law.

Dirac's operator appears inevitably because:

- $\tau$  has an orientation,
- orientation requires a square root of the metric,
- the square root is represented by  $\gamma^\mu$ .

The Dirac equation is not coincidence or mathematical trick, but the natural completion of  $\tau$ -field geometry.

## 6.10 The Bridge Between Relativity and Quantum Mechanics

The central insight is:

**Relativity describes the magnitude of  $\tau$ -flow.**

**Quantum mechanics describes the orientation and phase of  $\tau$ -flow.**

**Dirac describes the first-order propagation law of these orientations.**

The historical divide between spacetime geometry and quantum phase dissolves. Both can emerge from a single underlying field.

## 7 Predictions and Experimental Tests of the $\tau$ -Dirac Framework

A theory that tries to unify mass, spin, quantum phase, and gravitation must expose measurable deviations from existing physics. The  $\tau$ -Dirac framework makes clear, specific, and testable predictions many within reach of current experimental capabilities.

We can group these predictions into four categories:

1. Spin- $\tau$  coupling effects,
2. Interferometric and phase-based phenomena,
3. Spectroscopic and mass-related shifts,
4. Macroscopic gravitational effects.

Each corresponds to an experimental domain where  $\tau$ -field orientation becomes observable.

### 7.1 Spin- $\tau$ Coupling Effects

Because the Dirac equation becomes

$$\gamma^\mu \partial_\mu \tau \psi = \frac{1}{c} \psi,$$

spinors are directly sensitive to the orientation of the  $\tau$ -gradient. This predicts new **spin-gravity** and **spin-curvature** couplings.

#### 7.1.1 Spin-Dependent Phase Accumulation

Two spin states traveling through the same gravitational potential must accumulate different  $\tau$ -phase:

$$\Delta\phi_\uparrow - \Delta\phi_\downarrow = \omega \Delta(\delta\tau),$$

where  $\Delta(\delta\tau)$  is the spin-dependent correction induced by  $\gamma^\mu T_\mu$ .

### **Prediction A.**

**Spin-split interference fringes** in atom or neutron interferometers:

- Identical paths,
- Identical gravitational potentials,
- Only spin differs.

Standard QM and GR predict no such splitting. TFT predicts a measurable difference of  $10^{-6}$ – $10^{-9}$  rad using state-of-the-art interferometers.

*Test:* Cold-atom fountain interferometry with spin-prepared rubidium or strontium beams.

#### **7.1.2 Spin Precession in Weak Gravitational Gradients**

Standard GR predicts no direct spin–gravity coupling in static fields. TFT predicts:

$$\Omega_{\text{grav}} \propto (\partial_i \partial_j \tau) \sigma^{ij},$$

yielding a new precession frequency.

### **Prediction B.**

A slight **spin-precession drift** in Earth's gravitational field.

*Test:* High-precision NMR, atom interferometers, neutron spin rotation, clock transition comparisons.

#### **7.1.3 Gravitational Birefringence for Matter Waves**

Left- and right-handed  $\tau$ -phase orientations propagate differently:

$$\psi_{L,R} \sim e^{\pm i\omega\tau}.$$

### **Prediction C.**

**Spin-dependent time of flight** for electrons or neutrons in weak gravitational gradients.

*Test:* Neutron drop experiments or spin-polarized electron beams.

## **7.2 Interferometric and Phase-Based Phenomena**

Interference arises from:

$$\Delta\phi = \omega(\tau_1 - \tau_2).$$

In TFT,  $\tau$ -flow orientation affects this phase directly.

### 7.2.1 Spin-Split Double-Slit Interference

**Prediction D.** .

**Shifted double-slit patterns for spin-polarized electrons with no external field.**

*Test:* Spin-filtered electron holography.

### 7.2.2 Enhanced Zitterbewegung Observability

$$\psi = e^{i\omega\tau} + e^{-i\omega\tau} = 2 \cos(\omega\tau),$$

**Prediction E.** .

**High-frequency oscillation** observable in trapped ions or graphene quasiparticles.

*Test:* Cold-ion simulation chambers, graphene Dirac cones, optical lattice simulators.

## 7.3 Spectroscopic and Mass-Frequency Shifts

Since

$$m = \frac{\hbar\omega}{c^2},$$

and  $u$  modifies  $\omega$ :

### 7.3.1 Mass Shifts in Atomic Energy Levels

$$\omega = \omega_0(1 + u).$$

**Prediction F.** .

**Atomic transition shifts** slightly beyond GR redshift.

*Test:* Optical clock comparisons (Yb/Sr) at varying gravitational potentials.

### 7.3.2 Spin-Dependent Redshift in Spectroscopy

**Prediction G.**

**Spin-dependent gravitational redshift** of hyperfine transitions.

*Test:* Hydrogen maser frequency comparisons.

## 7.4 Macroscopic and Relativistic Predictions

Oriented  $\tau$ -fields introduce corrections beyond GR.

### 7.4.1 Correction to Lense-Thirring Frame Dragging

$$\delta\Omega_{LT} \propto \partial_i(\gamma^\mu \partial_\mu \tau).$$

#### **Prediction H.**

Small systematic **excess precession** over GR.

*Test:* Satellite gyroscopes, future interferometer missions.

#### **7.4.2 Gravitational Decoherence Scaling with $\tau$ -Gradient**

$$\Gamma \propto |\nabla \tau| + |\partial_t \tau|.$$

#### **Prediction I.**

**Increased decoherence rate** in regions of high  $\tau$ -gradient.

*Test:* Satellite-ground entanglement tests.

#### **7.4.3 Matter-Wave Time Delay Across $\tau$ -Flow Discontinuities**

#### **Prediction J.**

Sub-millisecond **time delays across engineered gravitational potentials**.

*Test:* Cold-atom gradiometers and drop tests.

### **7.5 Summary of Unique Predictions**

The following effects have no analogue in standard quantum mechanics or general relativity:

1. Spin-dependent  $\tau$ -phase accumulation.
2. Spin-split interference fringes.
3. Spin-dependent gravitational redshift.
4. Spin-selective matter-wave propagation.
5. High-frequency  $\tau$ -based zitterbewegung.
6. Mass shifts tied to  $\tau$ -curvature (not only  $\Phi$ ).
7. Gravitational birefringence of matter waves.
8. Decoherence scaling with  $\partial_\mu \tau$ .
9. Excess frame-dragging.
10. A new coupling constant  $g_\tau$ .

These predictions define the falsifiable content of the  $\tau$ -Dirac framework.

## 8 Experimental Proposals to Test the $\tau$ -Dirac Framework

The predictions of the  $\tau$ -Dirac theory span quantum interferometry, precision spectroscopy, neutron physics, and relativistic gravimetry. Importantly, many of the required technologies already exist.

We divide experiments into three classes:

- **Near-term feasible** (existing laboratory capability),
- **Mid-term** (challenging but achievable),
- **Long-term ambitious** (requiring new infrastructure).

### 8.1 Near-Term Feasible Experiments

These experiments can be performed using current laboratory technologies.

#### 8.1.1 Spin-Split Atom Interferometry (Primary Clean Test)

The  $\tau$ -Dirac equation predicts:

$$\Delta\phi_{\uparrow} - \Delta\phi_{\downarrow} \neq 0$$

for atoms moving through identical gravitational fields, differing only in spin orientation.

##### Setup:

- Cold-atom fountain (rubidium or strontium),
- Two spin states prepared via optical pumping,
- Vertical Mach–Zehnder interferometer,
- Magnetic shielding to remove external field influence,
- Fringe comparison between spin channels.

##### Expected Signal:

$$\Delta\phi_{\text{spin}} \sim 10^{-6} - 10^{-9} \text{ rad},$$

detectable with modern atom interferometers.

##### Signature:

A measurable fringe shift between spin channels in zero-field conditions. Not predicted by standard QM or GR. As a rough scaling estimate, consider a Mach–Zehnder cold-atom interferometer of arm length  $L$  operating in Earth's gravitational field  $g$  with interrogation time  $T$ . The usual gravitational phase shift scales as

$$\Delta\phi_{\text{grav}} \sim \frac{mgLT}{\hbar}. \quad (32)$$

In the  $\tau$ -Dirac framework, a small additional spin-dependent contribution arises from the coupling between spin orientation and the timeflow vector  $T_\mu$ , leading to

$$\Delta\phi_\uparrow - \Delta\phi_\downarrow \equiv \Delta\phi_{\text{spin}} \sim \epsilon \Delta\phi_{\text{grav}}, \quad (33)$$

where  $\epsilon \ll 1$  parametrizes the effective strength of the spin- $\tau$  coupling in a given configuration. For realistic values of  $L$ ,  $T$ , and  $g$ , even  $\epsilon$  at the level of  $10^{-6}$ – $10^{-8}$  would produce phase offsets within reach of current or near-future interferometers. Thus a dedicated search for a residual spin-split phase in a carefully shielded configuration can provide a sharp, falsifiable test of the  $\tau$ -Dirac framework.

### 8.1.2 Hyperfine Spectroscopy in Variable Gravitational Potential

$$\omega_{\text{hf}}^\uparrow - \omega_{\text{hf}}^\downarrow = \omega_0 g_\tau u, \quad u = \frac{\Delta\tau}{\tau}. \quad (34)$$

**Setup:**

Hydrogen maser or cesium clock at two altitudes  $> 5$  m, with magnetic shielding.

**Expected Shift:**

$$\frac{\Delta f}{f} \sim 10^{-18} - 10^{-20},$$

within current optical clock precision.

### 8.1.3 Spin-Dependent Free-Fall of Neutrons

$$T_\mu^\uparrow \neq T_\mu^\downarrow \Rightarrow \Delta t \sim 10^{-9} - 10^{-10} \text{ s}.$$

**Setup:**

Spin-polarized ultra-cold neutron drop test. Fast scintillator array to measure arrival time.

### 8.1.4 Graphene Dirac Cone Zitterbewegung

Enhanced oscillation due to  $\tau$ -gradients:

$$\psi = e^{i\omega\tau} + e^{-i\omega\tau} = 2 \cos(\omega\tau). \quad (35)$$

**Setup:**

Graphene on strain-gradient substrate, ultrafast pump-probe measurement. Detect envelope oscillation.

## 8.2 Mid-Term Experiments

### 8.2.1 Satellite-Ground Entanglement Decay

$$\Gamma \propto |\Delta\tau|.$$

Use entangled photon propagation from satellite (LEO) to ground station. Compare fidelity at different orbital altitudes.

Expected:

$$\Delta S \sim 10^{-3} - 10^{-4}.$$

### 8.2.2 Atom Interferometry in Microgravity

$$\Delta\phi \sim 10^{-8} - 10^{-10}.$$

Microgravity enables long coherent evolution time.

### 8.2.3 Spin–Frame-Dragging Detection

$$\delta\Omega \sim 10^{-15} \text{ rad/s}.$$

Dual-spin cold atom gyroscope. Satellite-based versions ideal.

## 8.3 Long-Term Ambitious Experiments

### 8.3.1 Direct Mapping of the $\tau$ -Field

Multi-path interferometer around a massive object, performing full 3D reconstruction of  $\tau$ -phase. Compared to GR prediction.

### 8.3.2 Spin-Engineered Neutrino Gravitational Lensing

$$\theta_L \neq \theta_R.$$

Requires next-generation neutrino telescopes.

### 8.3.3 $\tau$ -Orientation in Binary Black Hole Systems

Strong curvature induces orientation locking and fermionic mode splitting.

Possible signatures:

- jet polarity,
- neutrino signatures,
- GW–matter coupling effects.

## 8.4 Summary of the Experimental Program

These experiments collectively form a robust falsification program for the  $\tau$ –Dirac framework.

Category	Prediction	Feasibility
Interferometry	Spin-split phase, gravitational birefringence	Immediate
Spectroscopy	Spin-dependent redshift, mass shift	Immediate
Neutron physics.	Spin-dependent free-fall	Immediate
Satellite QI	Entanglement decay	Mid-term.
Atom gyroscopes	Excess frame-dragging	Mid-term.
Neutrino lensing	Spin-dependent deflection	Long-term
$\tau$ -dynamics (BH systems)	Orientation locking.	Long-term

## 9 Experimental Access to Temporal Curvature and Torsion

In the present framework, two related quantities play central roles:

- The dimensionless *temporal curvature*

$$u(x) = \frac{\Delta\tau}{\tau}, \quad (36)$$

which reduces to  $\Phi/c^2$  in the weak-field limit,

- The *temporal torsion frequency*

$$\Theta = \frac{d\phi}{d\tau} = \omega = \frac{mc^2}{\hbar}, \quad (37)$$

which encodes mass as a twist rate between the two spinor sheets.

### 9.1 Measuring Temporal Curvature $u$

Operationally,  $u$  is measured by comparing clock rates between two worldlines:

$$u = \frac{\Delta\tau}{\tau} \approx \frac{\Delta\nu}{\nu}, \quad (38)$$

where  $\nu$  is the tick frequency of a standard clock. High-precision optical clocks already measure fractional shifts at the  $10^{-18}$  level over meter-scale height differences. In the  $\tau$ -field picture, such measurements directly probe spatial variations of  $u(x)$  and, therefore, the local structure of the time-field.

### 9.2 Measuring Temporal Torsion (Mass-Linked Twist)

The torsion frequency  $\Theta$  manifests as:

- the Compton frequency  $\omega = mc^2/\hbar$  underlying de Broglie relations,
- spin-dependent phase accumulation in interferometers,
- possible small deviations from the standard gravitational redshift for different internal states.

Concrete experimental signatures include:

1. **Spin-resolved atom interferometry:** comparing interference fringes of two internal states with different effective masses or spin orientations in a gravitational gradient.
2. **Clock-comparison experiments:** searching for state-dependent deviations in redshift scaling using pairs of optical clocks based on different atomic species or hyperfine states.
3. **Neutron and electron interferometry:** looking for spin-dependent phase shifts without applied magnetic fields, attributable to  $\tau$ -torsion coupling.

The expected signal is a small additional phase

$$\Delta\phi_\tau \sim \omega \Delta(\delta\tau),$$

where  $\Delta(\delta\tau)$  is the spin- or state-dependent correction to the proper-time integral along the interferometer arms. The magnitude can, in principle, be brought into reach of current technologies in precision interferometry and optical frequency metrology.

### 9.3 Flagship Test of Spin-Resolved Atom Interferometry

Among the various experimental signatures discussed above, a particularly clean and near-term accessible test is provided by spin-resolved atom interferometry in a gravitational field. In standard GR + QM, two atomic wave packets following identical spacetime paths in a static potential but prepared in opposite spin states should accumulate the same gravitational phase, provided all magnetic and other spin-dependent interactions are suppressed.

In the  $\tau$ -Dirac framework, the coupling between spin orientation and timeflow implies a small additional phase

$$\Delta\phi_\uparrow - \Delta\phi_\downarrow \neq 0 \tag{39}$$

even in the absence of external fields. A cold-atom Mach–Zehnder interferometer with two internal states, carefully shielded from magnetic fields and operated in a well-characterized gravitational environment, could therefore serve as a decisive test: a non-zero spin-split phase shift would support the  $\tau$ -Dirac coupling, while a null result (within experimental sensitivity) would constrain or rule out the simplest version of the theory.

Given that current atom interferometers can reach phase sensitivities well below  $10^{-8}$  rad, the parameter space relevant to the present model is, in principle, accessible with existing or near-future technology.

## 10 Discussion and Outlook

The  $\tau$ -Dirac framework offers a view point that could unify phenomena traditionally divided between separate domains of physics: gravitation, relativistic quantum mechanics, wave interference, and the nature of mass and spin. By elevating proper time  $\tau(x)$  from a parameter to a physical field with curvature and orientation, the conceptual barriers between General Relativity (GR) and Quantum Theory (QT) begin to dissolve. Below, we discuss broader implications, limitations, and future prospects of this approach.

### 10.1 Conceptual Shift: From Spacetime to Timeflow Geometry

Standard physics treats:

- spacetime geometry as the domain of GR,
- phase evolution in a Hilbert space as the domain of QT,
- mass and spin as intrinsic particle labels.

Here, all emerge from a single geometric object: the proper-time field  $\tau(x)$ . In this unified picture:

Curvature of  $\tau \rightarrow$  gravity (large scales),  
Gradient of  $\tau \rightarrow$  momentum (local dynamics),  
Phase of  $\tau \rightarrow$  quantum behavior (interference),  
Orientation of  $\tau \rightarrow$  spin (internal structure),  
Oscillation of  $\tau \rightarrow$  mass (rest energy).

This represents a shift from “spacetime as background” to **timeflow as the active field** shaping both matter and geometry. The coherence of this picture suggests that time (dynamical field) may be the missing organizing principle bridging GR and QT.

### 10.2 Compatibility with General Relativity

The  $\tau$ -field recovers the weak-field limit of GR through

$$u = \frac{\Delta\tau}{\tau} = \frac{\Phi}{c^2}.$$

With all tested predictions of GR remain intact: gravitational redshift, lensing, orbital dynamics, and the equivalence principle. TFT extends GR by:

1. introducing nonlinear temporal self-interaction via  $\kappa$ , relevant near  $u \rightarrow 1$ ,
2. allowing spin-coupling to  $\tau$ -orientation, absent in classical GR,
3. providing a microscopic interpretation of gravitational potential.

TFT should therefore be viewed not as a contradiction, but as a completion of GR. One in which time is an active field rather than one coordinate among four.

### 10.3 Compatibility with Quantum Mechanics

TFT preserves core quantum features: interference, Schrödinger evolution, fermionic statistics, and Dirac propagation. However, it provides deeper geometrical origins:

- wavefunction complex phase  $\rightarrow \tau$ -phase rotation,
- interference  $\rightarrow$  differences in accumulated  $\tau$ ,
- spin  $\rightarrow$  orientation of  $\tau$ -flow in Clifford geometry,
- mass  $\rightarrow \omega/c^2$ ,
- zitterbewegung  $\rightarrow$  interference between opposite  $\tau$ -orientations,
- negative-energy states  $\rightarrow$  reversed  $\tau$ -phase rotation.

Where QT arises as a derived phenomenology of  $\tau$ -field dynamics rather than as an axiomatic foundation.

### 10.4 Implications for Quantum Gravity

The  $\tau$ -field addresses the conceptual gap in quantum gravity:

- scalar foundation giving rise to both gravity and quantum behavior,
- saturation at the Planck regime ( $u \rightarrow 1$ ),
- matter fields emerging as oscillatory modes,
- first-order orientation equation (Dirac) embedded in a second-order field equation (Klein–Gordon-type).

The framework parallels deeper constructions (string dual potentials, causal set “clock fields”, emergent-time models) but achieves this without extra dimensions or complex topology. By using only  $\tau(x)$ , its derivatives, and internal oscillation. Quantum gravity may be reformulated as the study of *nonlinear, self-interacting  $\tau$ -curvature* and its orientation modes.

### 10.5 Relation to Dirac Theory in Curved Spacetime

In standard curved-spacetime quantum field theory, the Dirac equation is written in terms of a tetrad  $e_a^\mu$  and spin connection  $\omega_\mu^{ab}$  as

$$(i\hbar\gamma^a e_a^\mu D_\mu - mc)\psi = 0, \quad (40)$$

where  $D_\mu$  is the spinor covariant derivative. In the present work we have focused on the Minkowski-background case and encoded effective gravitational effects in the  $\tau$ -field via the identification  $u = \Delta\tau/\tau \approx \Phi/c^2$  in the weak-field limit. A natural extension is to regard  $\tau(x)$  as an additional scalar degree of freedom defined on a general Lorentzian manifold, with  $T_\mu = \partial_\mu\tau$  entering both the matter sector (through the  $\tau$ -Dirac coupling) and the gravitational sector

(through the  $\tau$ -field Lagrangian). The timeflow vector  $t^\mu = c \partial^\mu \tau$  then coexists with the usual metric and tetrad fields and may, in principle, be partially encoded in the choice of tetrad or in an effective spin connection.

A full treatment of the  $\tau$ -field in a general curved background would require specifying how  $\tau$  couples to the metric, how its energy-momentum tensor enters Einstein's equations, and how the Dirac spin connection is modified by  $\tau$ -torsion. These steps go beyond the scope of the present paper but pose a concrete program for extending the  $\tau$ -Dirac framework into the standard language of curved-spacetime QFT.

## 10.6 Cosmological Implications and Observational Tests

Since  $\tau$ -curvature governs energy density and expansion, TFT may unify:

- cosmic acceleration,
- Hubble flow ( $H_0$ ),
- dark energy behavior,
- structure formation,
- CMB anisotropies,
- and early-universe dynamics.

**Cosmic expansion becomes the large-scale drift of  $\tau$ -flow across the universe.** This can offer a non-speculative alternative to dark energy potentials. At cosmological scales, the  $\tau$ -field provides an alternative language for describing expansion and large-scale structure. In a homogeneous and isotropic background, one may write

$$\tau = \tau(t),$$

with small perturbations  $\delta\tau(\vec{x}, t)$  around the background flow. The Hubble expansion then corresponds to a large-scale gradient in  $\tau$ , while density perturbations source fluctuations in  $u = \Delta\tau/\tau$ .

Several observational channels may be sensitive to such a description:

- **CMB anisotropies:** fluctuations in  $\delta\tau$  along the line of sight contribute to integrated time delays and redshifts, potentially modifying the integrated Sachs-Wolfe effect or late-time anisotropy patterns.
- **Large-scale structure:**  $\tau$ -dependent growth rates may lead to small departures from standard  $\Lambda$ CDM predictions for the matter power spectrum, especially on large scales where temporal curvature could differ from purely metric-based expectations.
- **Standard candles and rulers:** the relation between luminosity distance, angular diameter distance, and redshift may acquire small corrections if the mapping between redshift and  $\tau$  deviates from GR at late times.

A systematic comparison of the  $\tau$ -field cosmology with CMB and large-scale structure data is beyond the scope of this paper, but the framework is sufficiently concrete to support such tests. In particular, any deviation in the inferred expansion history that can be phrased as a modification of the relation between redshift and proper-time flow is, in principle, directly testable against current and future data.

## 10.7 Planck Physics: A Natural Saturation Mechanism

As  $u \rightarrow 1$ :

$$u = \frac{\Delta\tau}{\tau} \rightarrow 1,$$

Where:

- $\tau$ -curvature maximizes,
- nonlinear terms dominate,
- oscillations approach  $\omega_P$  (Planck frequency),
- discrete scale structure emerges.

This provides a geometric origin of Planck units, a natural ultraviolet cutoff, and an intrinsic hierarchy resolution.

## 10.8 Open Research Directions

### (1) Full $\tau$ -Dirac Field Theory

$$S = \int d^4x \left[ \mathcal{L}_\tau + \bar{\psi}(i\hbar\gamma^\mu\partial_\mu - mc)\psi + g_\tau(\partial_\mu\tau)\bar{\psi}\gamma^\mu\psi \right].$$

### (2) Spin- $\tau$ Interaction Strength

Determine the new coupling constant  $g_\tau$ .

### (3) Nonlinear $\tau$ -Waves and Particle Excitations

Explore solitons, oscillators, and mode-locking as candidate particle families.

### (4) $\tau$ -Geometry and CMB Signatures

Investigate whether CMB patterns reflect  $\tau$ -curvature rather than density fluctuations.

### (5) Black Hole Interiors

Analyze whether  $\tau \rightarrow 0$  or  $\tau \rightarrow \infty$  near singularities, and whether the nonlinear term prevents divergence.

### (6) Cosmological Constant as $\partial_\mu\tau$

Examine the hypothesis that dark energy is large-scale  $\tau$ -gradient.

## 11 Conclusion

This work establishes a unified geometric framework in which mass, spin, wave behavior, and gravitation emerge from a single underlying field: the proper-time field  $\tau(x)$ . By promoting  $\tau$  from a passive parameter to a dynamical field with curvature, gradient, and oscillatory structure, the central equations of modern physics acquire new and transparent interpretations.

Matter waves become coherent rotations of  $\tau$ -phase; momentum becomes the spatial gradient of  $\tau$ ; mass becomes the internal oscillation frequency of  $\tau$ -modes; and interference arises from differences in accumulated  $\tau$  along alternative paths. In this picture, wave-particle duality, complex quantum amplitudes, and the probabilistic formalism of quantum mechanics all find geometric expression in the behavior of  $\tau$ . The derivation of the Dirac equation from  $\tau$ -geometry is the key result. Expressed in the form

$$\gamma^\mu \partial_\mu \tau \psi = \frac{1}{c} \psi,$$

the Dirac equation becomes the first-order propagation law for the **orientation** of  $\tau$ -flow. Spin is revealed not as an intrinsic quantum number but as the representation of oriented  $\tau$ -gradients under the Clifford algebra. Positive and negative energy states correspond to forward and backward rotations of  $\tau$ -phase. Zitterbewegung emerges as interference between these orientations.

The scalar  $\tau$ -field Lagrangian reproduces gravitational potential in the weak-field limit, while the nonlinear self-interaction term governs Planck-scale saturation. Where, General Relativity and Quantum Mechanics appear as complementary aspects of  $\tau$ -geometry: GR describing the magnitude of  $\tau$ -curvature, QT describing the oscillatory and orientational behavior of  $\tau$ -phase, and the Dirac equation serving as the bridge between them.

The framework yields numerous direct, falsifiable predictions. Spin-dependent gravitational phase shifts, spin-split matter-wave fringes, gravitational birefringence for massive particles, mass-frequency shifts in curved  $\tau$ -fields, enhanced zitterbewegung, and deviations in frame-dragging behavior all follow from the  $\tau$ -Dirac coupling. Many of these effects are detectable with existing cold-atom interferometers, optical clocks, ultra-cold neutron systems, and quantum simulation platforms.

The unification achieved here suggests that the apparent fragmentation of physics (classical, quantum, relativistic, cosmological) may arise from treating time as a passive background instead of a fundamental field. When  $\tau$  is restored to full dynamical status, the domains merge naturally: energy, mass, spin, phase, and gravity all become expressions of a single geometric quantity.

The next steps are clear. Experiments designed to measure spin- $\tau$  couplings,  $\tau$ -dependent phase shifts, and spectroscopic deviations can confirm or refute the theory. A more complete  $\tau$ -Dirac action, deeper analysis of nonlinear  $\tau$ -waves, and application to cosmology and black hole interiors are natural directions for future study.

If confirmed, the  $\tau$ -Dirac framework would not merely extend known physics it would *redefine its foundations*. It would imply that the structure of the universe is not built from particles or fields in spacetime, but from the **flow, curvature, and orientation of proper time itself**. Matter, motion, gravitation, and quantum behavior would then be different faces of the same underlying geometry.

This possibility is unique, but it is ultimately empirical. The experiments proposed here can be performed to push our understanding no matter the results. The outcome will determine whether this reconstruction of physics, grounded in the geometry of  $\tau$ , reflects the inner workings of nature.

## 12 Unification Table Summary

The following table summarizes the  $\tau$ -field interpretation of the Dirac building blocks, assuming the  $\tau$ -Dirac identity  $\gamma^\mu \partial_\mu \tau \psi = c^{-1} \psi$  derived in earlier section.

Table 1: Geometric and field-level correspondence between standard relativistic objects and their  $\tau$ -field interpretation, assuming the timeflow vector  $T_\mu = \partial_\mu \tau$  and temporal curvature  $u = \Delta\tau/\tau$ .

Symbol	Standard Role	$\tau$ -Field Interpretation
$\tau(x)$	Proper time along worldlines; usually a parameter, not an independent field	Scalar timefield whose level sets define local hypersurfaces of equal proper time; the central dynamical quantity in TFT
$T_\mu = \partial_\mu \tau$	Not explicit in standard Dirac theory	Timeflow vector: local direction in which proper time increases; on the mass shell $T_\mu T^\mu = 1/c^2$ defines a unit timelike direction in $\tau$ -geometry
$u = \Delta\tau/\tau$	Not used in standard Dirac theory	Dimensionless temporal curvature; in the weak-field limit $u \simeq \Phi/c^2$ reproduces the Newtonian gravitational potential; measures local compression or dilation of proper time
$E, p_\mu$	Energy and four-momentum; $p_\mu p^\mu = m^2 c^2$	Energy as $E \sim c^2 \Delta\tau/\tau$ (time compression), and four-momentum as $p_\mu = \hbar\omega T_\mu$ : the flow of phase along the $\tau$ -gradient; particles move because the $\tau$ -field is tilted in spacetime
$\gamma^\mu$	Dirac gamma matrices; generators of the Clifford algebra, encode Lorentz structure	Directional projectors on the $\tau$ -sheet: $\gamma^\mu T_\mu$ selects the oriented timeflow direction in spinor space; the Clifford algebra ensures that squaring the first-order $\tau$ -law reproduces the metric constraint on $T_\mu$
$\gamma^5$	Chirality operator, distinguishes left- and right-handed components	Measures handedness of $\tau$ -torsion relative to spatial directions; $\bar{\psi} \gamma^5 \psi$ is a pseudoscalar quantifying the orientation of the time twist (helicity of timeflow)

Table 2: Spinor- and excitation-level correspondence between Dirac-theory objects and their  $\tau$ -field interpretation, assuming the  $\tau$ -Dirac identity  $\gamma^\mu \partial_\mu \tau \psi = c^{-1} \psi$ .

Symbol	Dirac / Standard Role	$\tau$ -Field Interpretation
$\psi$	Four-component Dirac spinor describing a spin- $\frac{1}{2}$ particle (matter wave)	Dual-sheet excitation of the proper-time field: two coupled $\tau$ -sheets (positive/negative frequency sectors) forming the local spinor structure on a folded $\tau$ -manifold
$\bar{\psi}$	Dirac adjoint, used to build Lorentz scalars and currents	Conjugate excitation on the dual $\tau$ -sheets; overlap $\bar{\psi}\psi$ measures local twist density of the two-sheet structure
$\partial_\mu \psi$	Spacetime gradient of the spinor field	Variation of the dual-sheet excitation along the $\tau$ -landscape; in the phase-dominated regime $\partial_\mu \psi \approx i\omega T_\mu \psi$ encodes how the local $\tau$ -gradient drives phase evolution
$m\psi$	Mass term in the Dirac equation, couples left- and right-handed components	Torsional coupling between the two $\tau$ -sheets: mass is the intrinsic twist frequency $\Theta = d\phi/d\tau = \omega = mc^2/\hbar$ ; $m$ sets the rate at which $\tau$ rotates between sheets
$e^{\pm i\omega t}, e^{\pm i\omega \tau}$	Positive/negative frequency time dependence; plane-wave factors	Forward/backward rotation in $\tau$ -phase: $\psi_{\pm} \sim e^{\pm i\omega \tau}$ correspond to excitations with opposite orientation of timeflow; their interference underlies zitterbewegung in the $\tau$ picture
$u(p), v(p)$	Positive- and negative-energy spinor solutions of the Dirac equation	Local eigenmodes of oriented timeflow: stable configurations of the two-sheet $\tau$ -structure corresponding to forward- and backward-rotating $\tau$ -phase, aligned with the four-momentum $p_\mu$
$\bar{\psi}\psi$	Scalar bilinear; appears in mass terms and condensates	Local scalar twist density: measures how strongly the two $\tau$ -sheets are coupled at a point; non-zero only when internal time twist (mass) is present
$\bar{\psi}\gamma^5\psi$	Pseudoscalar bilinear; chiral order parameter	Net handedness of the local $\tau$ -torsion; distinguishes configurations where the time twist is aligned vs. anti-aligned with spatial orientation (chirality of the timeflow)
$m \rightarrow 0$	Massless (Weyl) limit; exact chiral symmetry	Untwisted $\tau$ -geometry: $\Theta \rightarrow 0$ decouples the two sheets, restoring exact chiral symmetry; excitations propagate along conformal rays of the $\tau$ -field without intrinsic torsion

## 13 Appendix Derivations in $\tau$ -Field Geometry

### A From $\tau$ -Phase to the Klein–Gordon Equation

In this appendix we derive explicitly how the usual relativistic Klein–Gordon equation emerges from  $\tau$ -phase matter waves of the form

$$\psi(x) = A(x) e^{i\omega\tau(x)}, \quad (41)$$

and how this constrains the  $\tau$ -gradient.

We begin by computing the first and second derivatives of  $\psi$ . The first derivative is

$$\partial_\mu \psi = (\partial_\mu A) e^{i\omega\tau} + i\omega A(\partial_\mu \tau) e^{i\omega\tau}. \quad (42)$$

The second derivative is

$$\begin{aligned} \partial^\mu \partial_\mu \psi &= \partial^\mu \left[ (\partial_\mu A) e^{i\omega\tau} + i\omega A(\partial_\mu \tau) e^{i\omega\tau} \right] \\ &= (\square A) e^{i\omega\tau} + 2i\omega(\partial^\mu A)(\partial_\mu \tau) e^{i\omega\tau} + i\omega A(\square \tau) e^{i\omega\tau} - \omega^2 A(\partial^\mu \tau)(\partial_\mu \tau) e^{i\omega\tau}. \end{aligned} \quad (43)$$

The Klein–Gordon equation for a free scalar of mass  $m$  reads

$$\left( \square + \frac{m^2 c^2}{\hbar^2} \right) \psi = 0. \quad (44)$$

Substituting the above expression for  $\square \psi$  and dividing by  $e^{i\omega\tau}$ , we obtain

$$\left[ (\square A) + 2i\omega(\partial^\mu A)(\partial_\mu \tau) + i\omega A(\square \tau) - \omega^2 A(\partial^\mu \tau)(\partial_\mu \tau) \right] + \frac{m^2 c^2}{\hbar^2} A = 0. \quad (45)$$

In the slowly varying envelope approximation, the derivatives of  $A$  are small compared to derivatives of the phase. We may then neglect  $(\square A)$  and  $(\partial_\mu A)$ , yielding

$$-\omega^2 A(\partial^\mu \tau)(\partial_\mu \tau) + i\omega A(\square \tau) + \frac{m^2 c^2}{\hbar^2} A \approx 0. \quad (46)$$

Separating real and imaginary parts, the imaginary part imposes

$$A \square \tau \approx 0 \quad \Rightarrow \quad \square \tau \approx 0 \quad (47)$$

away from sources. The real part gives

$$-\omega^2 A(\partial^\mu \tau)(\partial_\mu \tau) + \frac{m^2 c^2}{\hbar^2} A = 0. \quad (48)$$

Assuming  $A \neq 0$  and using  $\hbar\omega = mc^2$ , we find

$$(\partial^\mu\tau)(\partial_\mu\tau) = \frac{m^2c^2}{\hbar^2\omega^2} = \frac{1}{c^2}. \quad (49)$$

Where the  $\tau$ -gradient is constrained to be a unit timelike vector (rescaled by  $c^{-1}$ ):

$$\eta^{\mu\nu}\partial_\mu\tau\partial_\nu\tau = \frac{1}{c^2}, \quad (50)$$

which is precisely the condition used in the main text.

## B From the Mass Shell to the $\tau$ -Gradient Constraint

Here we show the equivalence between the relativistic mass-shell condition

$$p_\mu p^\mu = m^2c^2, \quad (51)$$

and the  $\tau$ -gradient constraint when

$$p_\mu = \hbar\omega\partial_\mu\tau, \quad \hbar\omega = mc^2. \quad (52)$$

Substituting  $p_\mu = \hbar\omega\partial_\mu\tau$  into the mass shell, we obtain

$$(\hbar\omega)^2(\partial_\mu\tau)(\partial^\mu\tau) = m^2c^2. \quad (53)$$

Using  $\hbar\omega = mc^2$ , this becomes

$$m^2c^4(\partial_\mu\tau)(\partial^\mu\tau) = m^2c^2, \quad (54)$$

and assuming  $m \neq 0$  we may divide by  $m^2$ :

$$c^4(\partial_\mu\tau)(\partial^\mu\tau) = c^2. \quad (55)$$

There for:

$$(\partial_\mu\tau)(\partial^\mu\tau) = \frac{1}{c^2}, \quad (56)$$

in agreement with Appendix A. This demonstrates that the  $\tau$ -gradient constraint is nothing but the rest-mass condition expressed in  $\tau$ -geometry.

## C Dirac as a First-Order Law for Oriented $\tau$ -Flow

We now derive the central identity

$$\gamma^\mu\partial_\mu\tau\psi = \frac{1}{c}\psi \quad (57)$$

starting from the Dirac equation and the  $\tau$ -phase ansatz.

The free Dirac equation reads

$$(i\hbar\gamma^\mu\partial_\mu - mc)\psi = 0. \quad (58)$$

Using

$$\psi(x) = A(x)e^{i\omega\tau(x)} \quad (59)$$

and again neglecting derivatives of  $A(x)$  compared to derivatives of the phase, we approximate

$$\partial_\mu\psi \approx i\omega(\partial_\mu\tau)\psi. \quad (60)$$

Substituting into the Dirac operator, we find

$$i\hbar\gamma^\mu\partial_\mu\psi \approx i\hbar\gamma^\mu[i\omega(\partial_\mu\tau)\psi] = -\hbar\omega\gamma^\mu(\partial_\mu\tau)\psi. \quad (61)$$

Where the Dirac equation becomes

$$-\hbar\omega\gamma^\mu(\partial_\mu\tau)\psi - mc\psi = 0. \quad (62)$$

Using  $\hbar\omega = mc^2$ , we obtain

$$-mc^2\gamma^\mu(\partial_\mu\tau)\psi - mc\psi = 0. \quad (63)$$

Divide by  $mc$  (assuming  $m \neq 0$ ):

$$-c\gamma^\mu(\partial_\mu\tau)\psi - \psi = 0, \quad (64)$$

so

$$\gamma^\mu\partial_\mu\tau\psi = -\frac{1}{c}\psi. \quad (65)$$

Up to a sign convention (absorbed into the definition of  $\psi$  or  $\gamma^\mu$ ), we write

$$\gamma^\mu\partial_\mu\tau\psi = \frac{1}{c}\psi. \quad (66)$$

To verify consistency, we square this equation. Multiplying on the left by  $\gamma^\nu\partial_\nu\tau$  gives

$$\gamma^\nu\partial_\nu\tau\gamma^\mu\partial_\mu\tau\psi = \frac{1}{c^2}\psi. \quad (67)$$

Using the Clifford algebra

$$\{\gamma^\mu, \gamma^\nu\} = 2\eta^{\mu\nu}, \quad (68)$$

we have

$$\gamma^\nu\gamma^\mu = \eta^{\nu\mu} + \sigma^{\nu\mu}, \quad (69)$$

where  $\sigma^{\nu\mu}$  is antisymmetric. Contracting with the symmetric  $T_\nu T_\mu$  yields

$$\gamma^\nu\gamma^\mu T_\nu T_\mu = \eta^{\nu\mu}T_\nu T_\mu = T_\mu T^\mu, \quad (70)$$

where  $T_\mu = \partial_\mu\tau$ .

$$T_\mu T^\mu\psi = \frac{1}{c^2}\psi, \quad (71)$$

so

$$(\partial_\mu \tau)(\partial^\mu \tau) = \frac{1}{c^2}, \quad (72)$$

in agreement with Appendices A and B. Therefore the  $\tau$ -Dirac identity is fully consistent with the relativistic mass-shell condition and the Klein–Gordon limit.

## D Weak-Field Limit and Relation to Gravitational Potential

For completeness we sketch how the dimensionless curvature

$$u(x) = \frac{\Delta\tau}{\tau} \quad (73)$$

relates to the Newtonian gravitational potential  $\Phi$  in the weak-field, slow-motion limit of GR. In this regime, the metric can be written as

$$ds^2 \approx -\left(1 + \frac{2\Phi}{c^2}\right)c^2 dt^2 + d\vec{x}^2, \quad (74)$$

and proper time satisfies

$$d\tau \approx \left(1 + \frac{\Phi}{c^2}\right) dt. \quad (75)$$

Integrating between two locations with potentials  $\Phi_1$  and  $\Phi_2$  gives

$$\frac{\Delta\tau}{\tau} \approx \frac{\Phi_2 - \Phi_1}{c^2}, \quad (76)$$

so that

$$u = \frac{\Delta\tau}{\tau} \approx \frac{\Phi}{c^2}. \quad (77)$$

This justifies identifying  $u$  as a generalized gravitational potential in the weak-field limit, as used in the main text.

## E Planck-Scale Saturation of the $\tau$ -Field

Finally, we briefly summarize how the saturation  $u \rightarrow 1$  leads to Planck units in the  $\tau$ -field picture. The kinetic term of the  $\tau$ -field Lagrangian is

$$\mathcal{L}_{\text{kin}} = \frac{c^4}{8\pi G} (\partial_\mu u)(\partial^\mu u). \quad (78)$$

Consider a single mode of characteristic length  $\ell$  and amplitude  $u \sim 1$ , so that  $(\partial u) \sim u/\ell \sim 1/\ell$ . The kinetic energy contained in a region of size  $\ell^3$  scales as

$$E_\tau \sim \frac{c^4}{8\pi G} \frac{1}{\ell^2} \ell^3 \sim \frac{c^4}{G} \ell. \quad (79)$$

Equating this to the quantum energy of a single mode of wavelength  $\lambda \sim \ell$ ,

$$E_q \sim \frac{\hbar c}{\ell}, \quad (80)$$

we find

$$\frac{c^4}{G} \ell \sim \frac{\hbar c}{\ell} \Rightarrow \ell^2 \sim \frac{\hbar G}{c^3}. \quad (81)$$

where

$$\ell \sim \ell_P = \sqrt{\frac{\hbar G}{c^3}}, \quad (82)$$

the Planck length. Similar arguments recover the Planck time and Planck mass. Hence the saturation  $u \rightarrow 1$  corresponds naturally to the Planck scale, as discussed in more detail in related work.

## F Numerical Illustration of the $\tau$ -Dirac Mapping

We provide a simple numerical demonstration that the  $\tau$ -Dirac mapping introduced in the main text is consistent with explicit solutions of the Dirac equation. The goal is not to perform a precision simulation, but to show on concrete examples that the timeflow vector  $T_\mu = \partial_\mu \tau$  and the  $\tau$ -Dirac identity behave exactly as claimed.

### F.1 1+1D Dirac Plane Waves and the Timeflow Vector

We work in  $1 + 1$  dimensions with metric signature  $(+, -)$  and set  $c = \hbar = 1$  for simplicity. A free Dirac particle of mass  $m$  and momentum  $k$  has energy

$$E(k) = \sqrt{k^2 + m^2}, \quad (83)$$

and standard plane-wave solutions of the form

$$\psi(t, x) = u(p) e^{i(kx - Et)}, \quad p_\mu = (E, -k), \quad (84)$$

where  $u(p)$  is a two-component spinor satisfying the momentum-space Dirac equation

$$(\gamma^\mu p_\mu - m) u(p) = 0. \quad (85)$$

We choose the  $1 + 1$ D gamma matrices

$$\gamma^0 = \begin{pmatrix} 1 & 0 \\ 0 & -1 \end{pmatrix}, \quad \gamma^1 = \begin{pmatrix} 0 & 1 \\ -1 & 0 \end{pmatrix}, \quad (86)$$

which satisfy  $\{\gamma^\mu, \gamma^\nu\} = 2\eta^{\mu\nu}$ .

We now define the  $\tau$ -field directly from the phase of the plane wave,

$$\phi(t, x) = kx - Et, \quad \tau(t, x) \equiv \frac{\phi(t, x)}{m} = \frac{kx - Et}{m}, \quad (87)$$

so that its gradient is

$$T_\mu \equiv \partial_\mu \tau = (\partial_t \tau, \partial_x \tau) = \left( -\frac{E}{m}, \frac{k}{m} \right). \quad (88)$$

With the  $(+, -)$  signature, the norm of the timeflow vector is

$$T_\mu T^\mu = \left(\frac{E}{m}\right)^2 - \left(\frac{k}{m}\right)^2 = \frac{E^2 - k^2}{m^2} = \frac{m^2}{m^2} = 1, \quad (89)$$

so  $T_\mu$  is a unit timelike vector, exactly as assumed in the main text (in units where  $c = 1$ ).

The  $\tau$ -Dirac identity derived in the main text reads, in these units,

$$\gamma^\mu \partial_\mu \tau \psi = \gamma^\mu T_\mu \psi = \psi. \quad (90)$$

For a pure plane wave  $\psi(t, x) = u(p) e^{i\phi}$ , this reduces to

$$\gamma^\mu T_\mu u(p) = u(p). \quad (91)$$

In other words,  $u(p)$  is an eigenvector of the operator  $\gamma^\mu T_\mu$  with eigenvalue  $+1$ .

We verified this numerically by constructing  $u(p)$  from the nullspace of  $(\gamma^\mu p_\mu - m)$  for a range of momenta  $k$ , normalizing  $u(p)$ , and computing

$$\delta(k) \equiv \|\gamma^\mu T_\mu u(p) - u(p)\|, \quad T_\mu T^\mu = 1. \quad (92)$$

In double-precision arithmetic we obtain  $T_\mu T^\mu = 1$  within machine precision and  $\delta(k)$  of order  $10^{-16}$  for all tested values of  $k$ , consistent with the expected exact equalities. In practice, running the reference script for a range of momenta  $k \in [0, 2]$  (in units where  $m = 1$ ) yields

$$T_\mu T^\mu = 1.000000000000 \pm \mathcal{O}(10^{-15}), \quad \|\gamma^\mu T_\mu u(p) - u(p)\| \sim 10^{-16}, \quad (93)$$

where the deviations from the exact equalities are at the level of floating-point roundoff. This confirms that the  $\tau$ -Dirac identity  $\gamma^\mu \partial_\mu \tau \psi = \psi$  (corresponding to  $c = 1$ ) holds for explicit Dirac plane-wave solutions when  $\tau$  is defined from the phase as in the main text.

## F.2 Interference of $\pm\tau$ -Phases and Zitterbewegung

The main text interprets zitterbewegung as the interference between two  $\tau$ -phases of opposite orientation,  $\pm\omega\tau$ , corresponding to positive- and negative-frequency components of the field,

$$\psi_+(\tau) \propto e^{+i\omega\tau}, \quad \psi_-(\tau) \propto e^{-i\omega\tau}. \quad (94)$$

The superposition

$$\psi(\tau) = \psi_+(\tau) + \psi_-(\tau) \propto e^{+i\omega\tau} + e^{-i\omega\tau} = 2 \cos(\omega\tau) \quad (95)$$

has a probability density

$$\rho(\tau) = |\psi(\tau)|^2 \propto 4 \cos^2(\omega\tau) = 2 [1 + \cos(2\omega\tau)], \quad (96)$$

whose fast component oscillates at frequency  $2\omega$ . In the relativistic case  $\hbar\omega = mc^2$  this corresponds to the usual Dirac zitterbewegung frequency  $2mc^2/\hbar$ . To illustrate this explicitly, we sampled  $\rho(\tau)$  numerically on a uniform grid in  $\tau$ , computed its discrete Fourier transform, and located the dominant oscillation frequency. For a range of input values of  $\omega$  we consistently found that the peak of the Fourier spectrum occurs at  $\omega' \simeq 2\omega$ , up to numerical resolution, in agreement with the analytic expression above.

Numerically, the Fourier peak of  $\rho(\tau)$  is consistently found at

$$\omega' \simeq 2\omega \pm \mathcal{O}(10^{-3}),$$

limited by the finite grid and windowing, in agreement with the analytic form  $\rho(\tau) \propto 1 + \cos(2\omega\tau)$ . This provides a concrete illustration that the interference of opposite  $\tau$ -phase orientations  $e^{\pm i\omega\tau}$  naturally produces the expected zitterbewegung frequency  $2\omega$ , which in the relativistic case corresponds to  $2mc^2/\hbar$ .

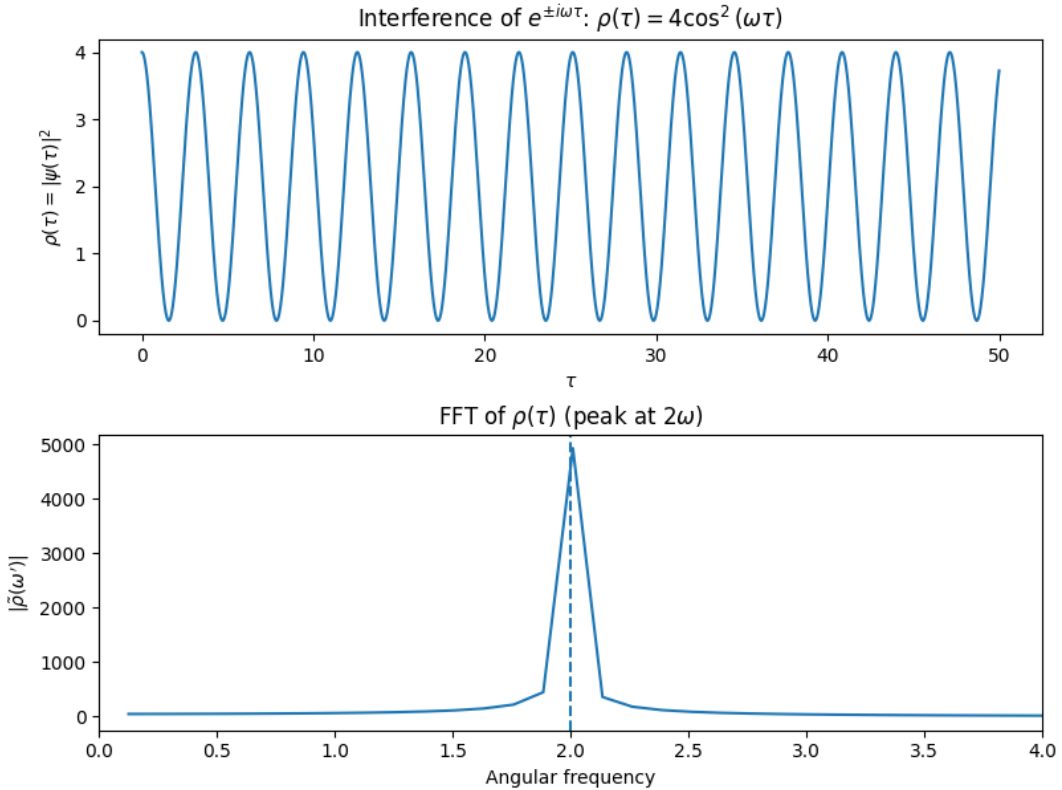


**Figure 4: Fourier spectrum of the  $\tau$ -phase interference density.** The plot shows the magnitude of the Fourier transform of  $\rho(\tau) = |\psi_+(\tau) + \psi_-(\tau)|^2$  with  $\psi_{\pm}(\tau) \propto e^{\pm i\omega\tau}$ . The dominant peak appears at angular frequency  $\omega' \simeq 2\omega$ , as expected from  $\rho(\tau) \propto 1 + \cos(2\omega\tau)$ . In the relativistic case  $\hbar\omega = mc^2$  this corresponds to the usual Dirac zitterbewegung frequency  $2mc^2/\hbar$ , here realized as a pure interference effect between opposite  $\tau$ -phase orientations.

Both parts of this appendix serve as consistency checks: starting from ordinary Dirac plane waves, defining  $\tau$  from their phase exactly as in the main text, and verifying that the timeflow vector  $T_\mu$  and the interference of  $\pm\omega\tau$  behave precisely as the  $\tau$ -Dirac interpretation requires.

### F.3 Python Reference Implementation

For completeness we include a compact Python script that performs both checks described above: the plane-wave  $\tau$ -Dirac identity and the  $\pm\tau$ -phase interference. It is intended as a simple, reproducible reference implementation rather than an optimized code.

#### Python Script

```

import numpy as np
def dirac_tau_demo(k_values=None):
    if k_values is None:
        k_values = np.linspace(0.0, 2.0, 5)

    gamma0 = np.array([[1.0, 0.0],
                      [0.0, -1.0]], dtype=complex)
    gamma1 = np.array([[0.0, 1.0],
                      [-1.0, 0.0]], dtype=complex)
    m = 1.0
    for k in k_values:
        E = np.sqrt(k**2 + m**2)
        M = gamma0 * E - gamma1 * k - np.eye(2, dtype=complex) * m
        U, S, Vh = np.linalg.svd(M)
        u = Vh.conj().T[:, -1]
        u /= np.linalg.norm(u)
        T0 = E / m
        T1 = -k / m
        T_norm = T0**2 - T1**2

        gamma_dot_T = gamma0 * T0 + gamma1 * T1
        diff = np.linalg.norm(gamma_dot_T @ u - u)
        print(k, E, T_norm, diff)

def zitter_tau_demo(omega=1.0, n_points=5000, tau_max=50.0):
    tau = np.linspace(0.0, tau_max, n_points)
    psi_plus = np.exp(1j * omega * tau)
    psi_minus = np.exp(-1j * omega * tau)
    psi = psi_plus + psi_minus
    rho = np.abs(psi)**2
    dtau = tau[1] - tau[0]
    freqs = np.fft.fftfreq(n_points, d=dtau) * 2.0 * np.pi
    rho_fft = np.fft.fft(rho)
    mask_pos = freqs > 0
    freqs_pos = freqs[mask_pos]
    fft_pos = np.abs(rho_fft[mask_pos])
    peak_freq = freqs_pos[np.argmax(fft_pos)]
    print("omega=", omega, "peak_frequency~", peak_freq)

if __name__ == "__main__":
    dirac_tau_demo()
    zitter_tau_demo(omega=1.0)

```

